

Effects of DEM resolution on modeling coastal flood vulnerability

Journal:	<i>Marine Geodesy</i>
Manuscript ID	UMGD-2018-0021.R2
Manuscript Type:	Research paper
Keywords:	Digital Elevation Model, Spatial Resolution, Structured Grid Models, Hydrodynamic Modeling, Coastal Flood Vulnerability Assessment

SCHOLARONE™
Manuscripts

Effects of DEM resolution on modeling coastal flood vulnerability

This paper examines whether DEM resolution affects the accuracy of predicted coastal inundation extent using LISFLOOD-FP, with application to a sandy coastline in New Jersey. DEMs with resolution ranging from 10 to 100 m were created using coastal elevation data from NOAA, using the North American Vertical Datum of 1988. A two-dimensional hydrodynamic flood model was developed in LISFLOOD-FP using each DEM, all of which were calibrated and validated against an observed 24-hour tidal cycle and used to simulate a 1.5 m storm surge. While differences in predicted inundated area from all models were within 1.0%, model performance and computational time worsened and decreased with coarser DEM resolution, respectively. This implied that using a structured grid model for modeling coastal flood vulnerability is based on two trade-offs: high DEM resolution coupled with computational intensity, but higher precision in model predictions, and vice versa. Furthermore, water depth predictions from all DEMs were consistent. Using an integrated numerical modeling and GIS approach, a two-scale modeling strategy, where a coarse DEM is used to predict water levels for projection onto a fine DEM was found to be an effective, and computationally efficient approach for obtaining reliable estimates of coastal inundation extent.

Keywords: Digital Elevation Model; Spatial Resolution; Structured Grid Models; Hydrodynamic Modeling; Coastal Flood Vulnerability Assessment.

1. Introduction

With anticipated rises in global sea-levels (Church *et al.* 2013; Jevrejeva *et al.* 2016; Waters *et al.* 2016) and the frequency of extreme storm surges (Grinsted *et al.* 2013; Lin and Emanuel 2015) under climate change, it is likely that the probability of flooding (McClatchey *et al.* 2014) will increase for low lying coastal areas (Bilskie *et al.* 2014; McGranahan *et al.* 2007). In turn, this will pose a significant threat to Small Island Developing States (SIDS) (Nicholls and Cazenave 2010), particularly those with densely populated coasts and an economic dependency on coastal tourism and natural resources. Thus, assessing coastal flood vulnerability, especially for small island states, is needed to guide coastal flood risk management. Two tools are commonly applied for these assessments: Geographic Information Systems (GIS) and hydrodynamic models. The former typically over-estimates flood extents due to issues relating to hydraulic connectivity, while the latter is generally more precise, but computationally demanding (Bates *et al.* 2005; Gallien *et al.* 2014; Seenath *et al.* 2016). This paper focuses on the application of hydrodynamic models for Coastal Flood Vulnerability Assessments (CFVA), specifically for cases where the outputs are to be used in informing coastal management initiatives.

Hydrodynamic models solve the Navier Stokes equations, the key equations of oceanic movements, by enforcing the laws of physics (Abbott and Basco 1989; Kantha and Clayson 2000). **Flow in hydrodynamic models is solved on either a structured or unstructured grid. The former imposes a finite difference approach to calculating flow, while the latter adopts a finite element or finite volume method (Bates and De Roo 2000; Spasojevic and Forrest 2008).** The main advantage of unstructured grid models is their triangular network, which increases their grid flexibility to resolve compound shorelines (Zhang and Baptista 2008). However, they are computationally intensive and sensitive to

numerical errors. Conversely, the key advantage of structured grid models is their short computational times (Horritt and Bates 2001b); however, they lack grid flexibility (Zhang and Baptista 2008). Therefore, intricate topographic and bathymetric features, characteristic of study sites, will not be fully accounted for when assessing coastal flood vulnerability using finite difference models (de Brye *et al.* 2010).

Due to a lack of grid flexibility, an issue surrounding the application of structured grid models is the selection of the spatial resolution of the DEM to be used in simulating coastal flood vulnerability, which may affect the accuracy and precision of model predictions. Unlike finite element models where the computational mesh can be modified to account for topographic and bathymetric complexities, grids used in finite difference models are fixed (i.e. a grid of square cells). Thus, it is likely that the accuracy of model outputs from fixed grid models can be affected by the resolution of the DEM used. Therefore, this paper assesses whether increasing DEM resolution in a structured grid flood model increases the accuracy of predicted coastal inundation extent, using LISFLOOD-FP with application to a sandy coastline in New Jersey (Figure 1), as a case study. The underlying aim of the study is to identify an optimal DEM resolution (if possible) for simulating coastal floods in a structured grid model, particularly for cases where the outputs are to support coastal management.

For logistical reasons, research in this paper is focused on a sandy coastline in New Jersey, where there is plentiful high-resolution elevation and coastal processes data, needed to effectively address the aim of the study. In addition, the New Jersey coastline selected has been affected by storm surges in the past (c.f. Colle *et al.* 2008), notably from Hurricane Sandy (Hall and Sobel 2013), and, therefore, presents an ideal case site for simulating coastal floods. Also, it is worth noting that this paper is not concerned with assessing the flood

vulnerability of a particular site, but rather on gauging the impacts of DEM resolution on simulating coastal floods. The outcomes of this research are likely to be useful in assisting coastal managers and modelers in data-poor, vulnerable coastal areas.

2. LISFLOOD-FP model specifications

LISFLOOD-FP is a simplified coupled 1D-2D finite difference model, based on a grid of square cells, developed by **Bates and De Roo (2000)**. A raster DEM and water inflow details are required by the model to simulate flood dynamics. Hydraulic continuity principles are applied in the model for the estimation of water depth in each cell of the DEM grid, and water routing across the floodplain is based on the difference in hydraulic head between adjacent cells (**Bates *et al.* 2005**). Flow rates in the model are estimated using the water surface height above land and the Manning friction coefficient (**Bates *et al.* 2005**).

In LISFLOOD-FP, change in water depth, h , in cell i, j is solved at time, t , using (Neal *et al.* 2011):

$$h_{i,j}^{t+\Delta t} = h_{i,j}^t + \Delta t \frac{Q_{xi,j-1}^t - Q_{xi,j}^t + Q_{yi,j-1}^t - Q_{yi,j}^t}{\Delta x^2} \quad (1)$$

where Δx is the cell width, Δt is the model time step, and Q^t is the flow between cells, calculated at the cell faces using a centered difference scheme decoupled in x or y directions using:

$$Q^t = \frac{q^t - gh_{flow}^t \Delta t \frac{\Delta(h^t+z)}{\Delta x}}{\left(1 + gh_{flow}^t \Delta t n^2 |q^{t-\Delta t}| / (h_{flow}^t)^{10/3}\right)} \Delta x \quad (2)$$

where:

- h_{flow} Depth between cells through which water can flow
- z Cell bed elevation
- n Manning’s roughness coefficient
- g Acceleration due to gravity
- q Flux between cells from the previous time-step (i.e. Q from the previous time step divided by cell width)

In LISFLOOD-FP, two-dimensional dynamic flows are represented on the floodplain by the discretization of floodplain flows over a regular grid. LISFLOOD-FP is designed for easy integration with a GIS for the purposes of the spatial representation of the output flood plain. The model has been validated and shown to perform well in coastal applications (Bates *et al.* 2005), and has been used by Lewis *et al.* (2013), Wadey *et al.* (2013), Quinn *et al.* (2014), and Seenath (2015), amongst others, for simulating coastal floods.

3. Methodology

The methodologies applied in this paper for running flood model simulations, validating model performance, and analyzing outputs are outlined across sections 3.1 to 3.5.

3.1 Data and model grids development

A post Hurricane Sandy coastal DEM of the application site, developed by the National Oceanic and Atmospheric Administration (NOAA), National Centers for Environmental Information (NCEI) (Eakins *et al.* 2015; N.C.E.I 2018), was used as the source data for the computational grid in LISFLOOD-FP (see Figure 2). This dataset provides a seamless integration of land topography and bathymetry created from a number of sources: NOAA Office of Coast Surveys, NOAA National Geodetic Survey, U.S. Geological Survey, and the

U.S. Army Corps of Engineers. The composed dataset has been obtained at a resolution of 1/9 arc second (~ 3 metres) and is referenced vertically and horizontally to the North American Vertical Datum of 1988 (NAVD 88), and the World Geodetic System (WGS) 84 datum in metres, respectively. To drive the flow in the model domain, tidal levels were obtained from NOAA's Atlantic City tide gauge station (Station ID: 8534720) (N.O.A.A 2018). The tidal levels were referenced to the same datum (horizontal and vertical) as the DEM, in metres.

Flood models, representative of the application site, were created using the LISFLOOD-FP code. This entailed the re-gridding of the source DEM into DEMs at varying grid resolutions: 10 m, 15 m, 20 m, 30 m, 40 m, 50 m, and 100 m. These formed the basis of the flood model domains representing the slope of the land and seabed at the study site. For resampling the source DEM, the nearest neighbour approach was used in ArcMap 10.3.1. As the nearest neighbour method is simply a relocation algorithm, it is often prone to deliver patchier results, which may affect modeling outcomes. Therefore, two smoothing algorithms (i.e. bilinear interpolation and cubic convolution) were used to transform the source DEM into a 30 m and 50 m DEM, to ascertain whether an alternative interpolation approach would have significantly altered the results of the nearest neighbour algorithm used.

3.2. Storm surge simulations and model calibration

A 1.5 m storm surge was superimposed onto a 24-hour tidal cycle, which was obtained from NOAA. The resulting time-series water levels (Figure 3) were entered along the east border in the boundary conditions file in LISFLOOD-FP. As a result, the storm surge was programmed in the model to approach the coast from an easterly direction. For flood simulations, a static friction value of 0.02 was used in the model, since this is the Manning's

friction coefficient for open water/sand (Mattocks and Forbes 2008), which broadly defines the study area. To verify the use of a friction value of 0.02, a model calibration was performed against an observed 24-hour tidal cycle (Figure 3) using friction values in the range of 0.01 to 0.04 at 0.005 intervals. Observations of the inland extent at high tide was extracted from a tide-coordinated, geo-referenced RapidEye image (6.5 m resolution), acquired from Planet (2017), by heads-up digitizing in ArcMap 10.3.1. Model performance in each friction test case was determined using the Root Mean Squared Error (RMSE) approach (equation 3) and a friction value of 0.02 was found to generate the best fit between the predicted and observed inland extent of the tide.

$$\text{RMSE} = \sqrt{\frac{\sum_{i=1}^N ((F_{[\text{Obs}],x} - F_{[\text{Pred}],x})^2 + (F_{[\text{Obs}],y} - F_{[\text{Pred}],y})^2)}{N}} \quad (3)$$

where $F_{[\text{Obs}]}$ is the observed flood points and $F_{[\text{Pred}]}$ is the corresponding closest computed flood position along the shoreline, each specified with locations with coordinates x, y , in metres UTM; N is the number of observations.

In the model, the acceleration solver was applied for calculating flow. The acceleration solver is a simplified form of the shallow water equations, where only the convective acceleration terms is assumed negligible. The flow between cells is calculated as a function of friction and water slopes, and local water acceleration. This approach is first-order in space and explicit in time but applies a semi-implicit treatment for the friction term to help stabilize the model. The time-step used in this solver varies throughout the simulation in accordance with the Courant-Friedrichs-Lewy (CFL) condition and is related to both cell size and water depth. For further details, see **Bates *et al.* (2013)**.

The key to selecting the storm surge level was to highlight the impact of DEM resolution on assessing flow in a variable topography. When superimposed onto the 24-hour tidal cycle selected, the highest water elevation generated was 1.92 m. The land areas within the immediate coastal zone ranges in elevation from around 0 to roughly 3.9 m (Figure 4). Though this is a relatively small variation, a 1.92 m water elevation (which represents roughly the midpoint between 0 and 3.9 m) will be able to show a more variable effect on water flow relative to using a larger or smaller storm surge level. Thus, differences (if any) in flood extent predicted from the re-gridded DEMs would be clearly shown with a 1.5 m storm surge. In addition, a 1.5 m storm surge falls within the range of highest water levels generated from previous storms at the study site (Colle *et al.* 2008). Therefore, the use of a 1.5 m storm surge enabled a realistic simulation of coastal floods for the application site.

3.3. Flood extent predictions

Hydrodynamic flood simulations were carried out in LISFLOOD-FP for the full 24-hour tidal cycle representing the abovementioned storm surge scenario, using each re-gridded DEM. The maximum water depth raster output from each simulation was analyzed in ArcMap 10.3.1. A depth threshold of 0.1 m was used to distinguish between flooded and non-flooded areas, since flood depths below this level is expected to exert very little consequence and, therefore, provide an extreme indication of flood extents which may be inappropriate and misleading (Aronica *et al.* 2002). Flood extent predictions obtained was used to create a flood extent map to highlight the impact of DEM resolution on predicted coastal inundation extent (see Figure 5).

3.4. Model validation

To add certainty to the modeling results and to ascertain the impact of DEM resolution on model accuracy, the flood models created from each re-gridded DEM were validated against an observed 24-hour tidal cycle, due to the absence of flood data for the application site. To facilitate this, observations of the inland extent at high tide was extracted from a tide-coordinated, geo-referenced RapidEye image (6.5 m resolution), acquired from Planet (2017), by heads-up digitizing in ArcMap 10.3.1. The corresponding observed 24-hour tidal cycle (Figure 3) was entered along the east border in the boundary conditions file in LISFLOOD-FP, as before. A simulation of the tidal cycle was carried out using each re-gridded DEM, and the projected inland extent of the tide from all models were found using a depth threshold of 0.1 m, as before. The distance between the observed and projected flood extents were calculated using the spatial analyst function ‘near’ in ArcMap 10.3.1, and the values obtained were used to estimate the RMSE (equation 3) in flood extent predictions from each re-gridded DEM.

More specifically, the inundation extent (i.e. the landward extent of the water boundary) was converted to points. The number of points is related to the DEM resolution from which they have been extracted, and ranges from 186 (from the 100 m re-gridded DEM) to 1923 (from the 10 m re-gridded DEM). These points were subsequently used to determine the offset between the observed flood extent line and predicted flood extent points. In ArcGIS, the shortest distance from a point to a line segment is the perpendicular to the line segment (see Figure 6). The distance between the predicted and observed flood extent indicators was used to estimate the RMSE of flood extent predictions from each re-gridded DEM.

3.5. Integrating numerical modeling and GIS for predicting coastal flood extent

To account for relevant details on coastal elevation, whilst ensuring computational efficiency and precision in coastal flood extent predictions, running structured grid, raster-based models with a coarse DEM and re-projecting the predicted water levels onto a fine DEM is worth considering. To explore this, water levels predicted for the observed 24-hour tidal cycle using the 15 m, 20 m, 30 m, 40 m, 50 m, and 100 m DEMs were projected onto the 10 m DEM. In particular, the maximum water depth raster output from the coarser DEMs were resampled to 10 m resolution and then subtracted from the 10 m DEM in ArcMap 10.3.1. As before, a 0.1 m depth threshold was used to delineate the predicted inundation extent from the resulting raster outputs, and their RMSE estimated using equation 3.

4. Results and analysis

The outputs from the re-gridding procedure, flood simulations, and model evaluations are presented across sections 4.1 to 4.3.

4.1. Spatial differences in elevation between re-gridded DEMs

From Table 1 and Figures 7-8, it would appear that the nearest neighbour re-sampling process did not significantly alter the quality and topographic complexity of the DEMs. This is ascertained by a Kruskal Wallis test, which indicated that there was no significant difference in the elevations between the re-gridded DEMs ($\chi^2 = 12.59$, $p = 1.000$). By resampling a fine resolution DEM using the nearest neighbour approach, the high-quality measurements are usually preserved, although they are spread out with greater point-to-point differences. Therefore, no significant differences between the re-gridded DEMs were expected. In real-world modeling applications, it is possible that a poorer quality DEM may be used from the beginning, the results of which can be starkly different. However, many high-quality datasets

are now becoming increasingly available through open-source repositories. Thus, the probability of obtaining high-resolution datasets is high relative to a few years ago.

Furthermore, a comparison of the 30 m and 50 m DEMs generated from the nearest neighbour, bilinear, and cubic convolution algorithms revealed no differences (Figure 9). Therefore, the flood model outputs derived from the nearest neighbour re-sampled DEMs is not likely to differ from those that would have been produced using a bilinear or cubic convolution smoothing algorithm.

4.2. Flood extent predictions relative to DEM resolution

Irrespective of spatial resolution, differences in the projected percentage of inundated area from all DEMs used in modeling the 24-hour tidal cycle and storm surge scenario were within 1.0% (Table 2). This suggest that coastal flood extent predictions from all re-gridded DEMs were consistent, as also illustrated in Figure 5. While the aerial change may seem small, the average distance between the observed and projected flood extents were not. From Table 3, it is noted that the modeled boundaries became further away from the true flood boundaries with decreasing grid resolution. This aligns with the model validation results, which indicated that LISFLOOD-FP’s performance worsened with coarsening DEM resolution (Table 3 and Figure 10). The small aerial changes in flood extent predictions is likely related to the steep terrain at the inundated in-land areas (see Figure 4). Had the terrain been flatter, it is likely that there would be larger differences between the models.

From Figure 4, much of the land at the study site varies within 4 m above NAVD88, whereas coastal profiles are relatively steep. In addition, there is an area of steep depression further inland due to the passage of a water course linked to a coastal lagoon. Therefore, the study site is characterized by steep depressions at the inundated in-land and beach areas, and

1
2
3 irregular slopes in the land areas. Thus, the topographic features, in particular the steep
4
5 depressions, is the key control of flood flow at the study site. For the representation of
6
7 depressions governing flood dynamics, nearest neighbour resampling is generally useful
8
9 (Casas *et al.* 2006; J. Zhang *et al.* 2014). As such, a coarse DEM would have represented the
10
11 key elevation characteristics of the study site well, leading to a good agreement between the
12
13 flood extent observation and predictions from each re-gridded DEM. In a geomorphological
14
15 setting where coastal floods are primarily controlled by small features such as groynes and
16
17 breakwaters, interpolation at low spatial resolution can exclude these features from the DEM
18
19 leading to flood extent over-estimation (c.f. Falter *et al.* 2013).
20
21
22
23

24 From Table 3 and Figure 10, it is acknowledged that the 10 m and 100 m grid DEM, i.e. the
25
26 finest and coarsest resolutions used, resulted in the lowest (29.08 m) and highest (90.28 m)
27
28 RMSE, respectively. Typically, RMSE values closer to 0 infer good model performance.
29
30 However, in this case study, roughly 29 m was the lowest RMSE generated from using a 10
31
32 m grid DEM. A potential reason behind this large error value is the uncertainty associated
33
34 with the horizontal and vertical accuracy of the DEM used. As the source DEM used was a
35
36 collection of multiple datasets, a quantitative assessment of its accuracy (horizontal and
37
38 vertical) was not estimated by the NCEI. Further, with the absence of ground control points,
39
40 the quality of the DEM could not have been assessed. But, as this study is primarily
41
42 concerned with illustrating the impact of DEM resolution on projections of coastal inundation
43
44 extent, the accuracy and precision of the DEM used is of little significance and consequence
45
46 relative to the study's findings. The paper is simply designed to guide coastal managers and
47
48 coastal flood modelers of the relevance (or non-relevance) of DEM resolution in coastal flood
49
50 modeling.
51
52
53
54
55
56
57
58
59
60

Regarding computational costs, the time taken to complete a 24-hour tidal cycle using a 10 m grid DEM was approximately 1 hour, while those carried out with lower DEM resolutions (15 m, 20 m, 30 m, 40 m, and 50 m) took less than 15 minutes. In both cases, the time taken to complete a 24-hour simulation was not excessive. This is due to the small area focused on in this study (i.e. a DEM equivalent to 29.62 km² (11.44 mi²)). For a larger area, such as the U.S. east coast, model run times using both fine (e.g. 10 m) and low resolution (e.g. 100 m) would be excessively longer.

4.3. Flood predictions from the integrated numerical modeling and GIS approach

To circumvent the issues associated with DEM resolution and computational intensity, whilst ensuring reasonable accuracies of flood extent predictions, an integrated numerical modeling and GIS approach was explored, as outlined in section 3.5. From Figure 10, a decrease in RMSE values was acquired from re-projecting the predicted water levels obtained from the coarser DEMs onto the 10 m DEM (i.e. the finest resolution used in this paper). This reflected a significant improvement in coastal flood extent predictions. Also, it insinuates that the lower resolution DEMs (15 m, 20 m, 30 m, 40 m, 50 m, and 100 m) were effective in predicting reasonably good and consistent water levels relative to the 10 m DEM. In turn, this made a more detailed demarcation of probable coastal flood extent possible with a higher resolution DEM at low computational costs.

5. Discussion

Results imply that selecting a DEM resolution for use in a structured grid coastal flood model is based on two trade-offs:

- (1) High DEM resolution coupled with long computational times, but higher precision in flood extent prediction. Ideally, this scenario is recommended for small geographical areas, where detailed studies is required for obtaining results with precision, and reasonable certainty that can be used for decision making in coastal management (Chen and Liu 2014; Hartnett and Nash 2017; Seenath *et al.* 2016). Namely, this option is recommended for local natural resource management agencies and environmental firms tasked with the job of managing small coastal areas of economic importance (e.g. beaches and coastal resorts), which are likely to be adversely affected by storm surges and sea-level rise under climate change.
- (2) Low DEM resolution coupled with short computational times, but lower precision in flood extent predictions. This option can facilitate the assessment of larger geographical areas (e.g. regional scales), but simulated outputs may contain questionable uncertainty and accuracy (Falter *et al.* 2013; Seenath *et al.* 2016). However, a coarse DEM can be used to provide a generalized indication of flood vulnerable areas in order to identify critical coastal areas (Gesch 2009) for a detailed assessment of coastal flood vulnerability to inform appropriate measures of coastal management.

From Figure 5, it is acknowledged that model predictions of flood extent matched relatively well irrespective of DEM resolution, but this can be linked to the elevation characteristics of the site (Li and Wong 2010). If an area is mainly flat or high, the DEM resolution used to simulate coastal floods may have little significance in terms of water level, but it can affect the horizontal position of the predicted flood boundary (Falter *et al.* 2013). In such geomorphological environments, small features (e.g.

depressions, narrow channels, and flood defenses) may have a more influential effect on flood flow, which may be excluded from a coarse DEM (Li and Wong 2010; Vaze *et al.* 2010) leading to poor predictions in horizontal flood boundary (Falter *et al.* 2013). Conversely, in a geomorphology with variable topography, characterized by large areas with steep and irregular slopes (i.e. a more rugged terrain), the elevation characteristics of the area would exert a more significant control on flood flow (c.f. Li and Wong 2010) than small features. Topographic features are generally well preserved by nearest neighbour resampling (Casas *et al.* 2006; Nikolakopoulos *et al.* 2006; J. Zhang *et al.* 2014), provided that the scale of the terrain characteristics is good enough relative to the resolution at which the DEM is being resampled to (Savage *et al.* 2016). In these cases, a coarse DEM may be suitable for simulating coastal floods. As aforementioned, the main control on flood flow at the study site is its topographic features. Therefore, a coarse DEM (resampled from a high-quality DEM) would have represented the key elevation characteristics of the study site well, leading to a good agreement between flood extent observation and predictions from each re-gridded DEM.

However, the accuracies inherent in the outputs acquired from the lower resolution DEMs were too low to be used for decision making in coastal management. Low spatial resolution means less detail (Li and Wong 2010; Savage *et al.* 2016; Vaze *et al.* 2010). Therefore, less detail will lead to simulated outputs farther away from reality (c.f. Falter *et al.* 2013). In the case of the application site, there were prominent slope characteristics which governed the flow of floods. In such cases, coarser DEMs will produce similar outputs as finer DEMs (see Figure 5). However, in a geomorphological setting where coastal floods are primarily controlled by small features such as groynes

and breakwaters, interpolation at low spatial resolution can exclude these features from the DEM leading to flood extent over-estimation (Falter *et al.* 2013; Savage *et al.* 2016). Repercussions of flood extent over-estimation include:

- (a) An over-exaggeration of flood zones, which can lead to the needless relocation of people (i.e. forced migration) (Seenath *et al.* 2016).
- (b) Waste of investment (Saghafian *et al.* 2013), particularly for persons paying high premiums to live in misguided flood risk zones (Mennel 2014).
- (c) Restricting development to non-flood zone areas, thus rendering potential valuable land as useless if it falls within a pseudo 'flood zone', leading to a probable loss in economic opportunities (Viglione *et al.* 2014).

Furthermore, modeling results suggests that fine DEMs (≤ 10 m) is perhaps best for modeling coastal flood vulnerability, since the finest DEM used (i.e. 10 m) generated the best fit between the flood extent predictions and observations. Attempts were made to run the model using a DEM with 5 m and 7 m resolution, but this was not computationally practical. Hydrodynamic models calculate flow per grid cell. Therefore, the finer the resolution, the longer the computational run time. Flood modeling in this paper was restricted to a coastal area the size of 29.62 km², which is small compared to coastal regions elsewhere. For larger geographical areas, a 10 m resolution may not be practical for reasons aforementioned. However, it is important to consider that the underlying purpose of any CFVA is often flood risk management. Thus, sufficient detail and precision in data inputs is needed for a realistic estimate of coastal flood vulnerability, particularly for areas with complex topographic and bathymetric features.

From Figure 10, the decrease in RMSE values acquired from re-projecting the predicted water levels obtained from using a coarser DEM onto a fine DEM reflected a significant improvement in coastal flood extent predictions. Also, it insinuated that the coarser DEMs (15 m, 20 m, 30 m, 40 m, 50 m, and 100 m) were effective in generating reasonably good and consistent water levels relative to the 10 m DEM. In turn, this made a more detailed demarcation of probable coastal flood extent possible with a higher resolution DEM, which can be useful for informing coastal flood risk management. This finding suggests that a two-scale modeling strategy, where (1) a coarse DEM is used to predict water levels and (2) a fine DEM is applied to transform the predicted water levels into a precise estimate of coastal inundation extent, is perhaps the best approach for modeling (and quantifying) coastal flood vulnerability.

Several river-based studies have shown that coarse DEMs can predict reasonably good water levels (Brandt 2016; Casas *et al.* 2006; Horritt and Bates 2001a), which can be used in flood analysis alongside DEMs of high quality (Horritt and Bates 2002). Therefore, the two-scale modeling strategy outlined is not new in modeling river floods, but rather commonly adopted in related river literature. However, in the coastal literature, flood modeling studies are either based on (1) the traditional raster-based modeling using a GIS, where land elevation lower than the elevation of floodwater at some level is considered flood-vulnerable, irrespective of hydraulic connectivity (i.e. the bathtub approach) or (2) hydrodynamic modeling, where the detailed physics behind the flood flow is simulated (Haer *et al.* 2018; Seenath *et al.* 2016). The former is more popular and widely adopted in related coastal literature (Gesch 2009; Haer *et al.* 2018; Leon *et al.* 2014), despite the many limitations associated with its simplistic approach towards CFVA (Kumbier *et al.* 2018; Leon *et al.* 2014; Seenath *et al.* 2016). Numerical raster-based modeling, where a DEM is used to simulate coastal floods in a

hydrodynamic model, is a fairly recent development in the coastal literature (Vousdoukas *et al.* 2016), and is sporadically used for coastal flood modeling relative to the bathtub approach. Therefore, while the outlined two-scale modeling strategy is very well-adopted in the river literature, it is not a strategy that has yet been extensively explored in related coastal literature. Thus, the outcomes of this study can lead to further considerations in integrating raster-based numerical models with a GIS for simulating coastal floods at large spatial scales at low computational costs, in order to better assess flood vulnerability for informing coastal management.

Figure 10 also illustrates that variations in RMSE values (though small) were obtained when predicted water levels from coarsening DEM resolution was projected onto the 10 m DEM. This suggest that DEM resolution do exert some level of influence on model accuracy. For example, RMSE values increased by 7.0% from projecting water levels predicted from a 100 m DEM relative to a 20 m DEM onto the 10 m DEM. This imply that some level of computational intensity is needed. As the underlying purpose of CFVA is often to inform coastal flood risk management, precision in model outputs is needed, since flood extent over-estimation can lead to over-management of coastal areas with adverse implications, as previously noted. In addition, flood extent underestimation can lead to the under-management of coastal environments, which can increase the risks associated with coastal hazards with adverse economic (e.g. infrastructural damage from storm surges), social (e.g. destruction of property and loss of livelihood from coastal floods) and environmental (e.g. weakening of natural defense systems, such as coastal dunes, from sediment redistribution by coastal floods) implications (Rosner *et al.* 2014; Siegrist and Gutscher 2006; Verwaest *et al.* 2012). Therefore, even though an option exists to use a two-scale modeling strategy for obtaining a reasonable estimate of coastal flood vulnerability at low computational costs, the

optimal lowest DEM resolution should be carefully selected based on site characteristics. In other words, the grid resolution of the input DEM should be fine enough to account for the main features of the area of interest.

6. Conclusions

This paper attempted to explore the effects of DEM resolution on modeling coastal flood vulnerability, using a raster-based, structured grid model, LISFLOOD-FP, with application to a sandy coastal stretch in New Jersey. The key conclusions drawn are:

1. The application of a structured grid, raster-based model for CFVA is based on two trade-offs: high DEM resolution coupled with long computational times, but higher precision, and vice versa. The former is more applicable for small geographical areas of economic importance (e.g. beaches) where high precision in model outputs is needed for flood risk management purposes, while the latter is more suitable for larger geographical areas (e.g. regional scales) where an indication of potential flood vulnerable areas is desired.
2. A two-scale modeling strategy, where (1) a coarse DEM is used to predict water levels in a numerical model and (2) a fine resolution DEM is used to transform the predicted water levels into a precise estimate of coastal flood extent within a GIS, appears to be an effective and computationally efficient approach for modeling, predicting, and quantifying coastal flood vulnerability.
3. As the underlying purpose of CFVA is often to inform coastal flood risk management, precision in model outputs is needed, since flood extent over- and under-estimation can lead to over- and under-management of coastal areas, respectively, with adverse implications. Therefore, while reasonable estimates of inundation extent can be

achieved at low computational costs by projecting predicted water levels from a coarse DEM onto a fine DEM, the optimal (lowest) DEM resolution should be carefully selected to ensure that the main elevation features of the area of interest are aptly represented in the model.

Acknowledgments

The use of LISFLOOD-FP (available from: <http://www.bristol.ac.uk/geography/research/hydrology/models/lisflood/>) is gratefully acknowledged. Sincerest thanks to the reviewers for their insightful comments in helping to improve the overall quality of the manuscript.

References

- Abbott, M.B. and D.R. Basco. 1989. *Computational fluid dynamics: An introduction for engineers*: Longman Scientific & Technical. <https://books.google.co.uk/books?id=GqYeAQAAIAAJ>
- Aronica, G., P.D. Bates and M.S. Horritt. 2002. Assessing the uncertainty in distributed model predictions using observed binary pattern information within glue. *Hydrological Processes* 16, no 10: 2001-16.
- Bates, P.D., R.J. Dawson, J.W. Hall, M.S. Horritt, R.J. Nicholls, J. Wicks and H. Mohamed Ahmed Ali Mohamed. 2005. Simplified two-dimensional numerical modelling of coastal flooding and example applications. *Coastal Engineering* 52, no 9: 793-810.
- Bates, P.D. and A.P.J. De Roo. 2000. A simple raster-based model for flood inundation simulation. *Journal of Hydrology* 236, no 1: 54-77.
- Bates, P.D., M. Trigg, J. Neal and A. Dabrowa. 2013. Lisflood-fp user manual code release 5.9.6. United Kingdom: University of Bristol.
- Bilskie, M.V., S.C. Hagen, S.C. Medeiros and D.L. Passeri. 2014. Dynamics of sea level rise and coastal flooding on a changing landscape. *Geophysical Research Letters* 41, no 3: 927-34.
- Brandt, S.A. 2016. Modeling and visualizing uncertainties of flood boundary delineation: Algorithm for slope and dem resolution dependencies of 1d hydraulic models. *Stochastic Environmental Research and Risk Assessment* 30, no 6: 1677-90.

- Casas, A., G. Benito, V.R. Thorndycraft and M. Rico. 2006. The topographic data source of digital terrain models as a key element in the accuracy of hydraulic flood modelling. *Earth Surface Processes and Landforms* 31, no 4: 444-56.
- Chen, W.-B. and W.-C. Liu. 2014. Modeling flood inundation induced by river flow and storm surges over a river basin. *Water* 6, no 10: 3182-99.
- Church, J.A., P.U. Clark, A. Cazenave, J.M. Gregory, S. Jevrejeva, A. Levermann, M.A. Merrifield, G.A. Milne, R.S. Nerem, P.D. Nunn, A.J. Payne, W.T. Pfeffer, D. Stammer and A.S. Unnikrishnan. 2013. Sea level change. In *Climate change 2013: The physical science basis. Contribution of working group i to the fifth assessment report of the intergovernmental panel on climate change*, eds Stocker, TF, Qin, D, Plattner, G-K, Tignor, M, Allen, SK, Boschung, J, Nauels, A, Xia, Y, Bex, V and Midgley, PM, 1137–216. Cambridge, United Kingdom and New York, NY, USA: Cambridge University Press.
- Colle, B.A., F. Buonaiuto, M.J. Bowman, R.E. Wilson, R. Flood, R. Hunter, A. Mintz and D. Hill. 2008. New york city's vulnerability to coastal flooding. *Bulletin of the American Meteorological Society* 89, no 6: 829-42.
- De Brye, B., A. De Brauwere, O. Gourgue, T. Kärnä, J. Lambrechts, R. Comblen and E. Deleersnijder. 2010. A finite-element, multi-scale model of the scheldt tributaries, river, estuary and rofi. *Coastal Engineering* 57, no 9: 850-63.
- Eakins, B.W., J.J. Danielson, M.G. Sutherland and S.J. Mclean. 2015. A framework for a seamless depiction of merged bathymetry and topography along u.S. Coasts. Paper presentat at the U.S. Hydro Conference, in National Harbor, Maryland.
- Falter, D., S. Vorogushyn, J. Lhomme, H. Apel, B. Gouldby and B. Merz. 2013. Hydraulic model evaluation for large-scale flood risk assessments. *Hydrological Processes* 27, no 9: 1331-40.
- Gallien, T.W., B.F. Sanders and R.E. Flick. 2014. Urban coastal flood prediction: Integrating wave overtopping, flood defenses and drainage. *Coastal Engineering* 91: 18-28.
- Gesch, D.B. 2009. Analysis of lidar elevation data for improved identification and delineation of lands vulnerable to sea-level rise. *Journal of Coastal Research* 10053: 49-58.
- Grinsted, A., J.C. Moore and S. Jevrejeva. 2013. Projected atlantic hurricane surge threat from rising temperatures. *Proc Natl Acad Sci U S A* 110, no 14: 5369-73.
- Haer, T., W.J.W. Botzen, V. Van Roomen, H. Connor, J. Zavala-Hidalgo, D.M. Eilander and P.J. Ward. 2018. Coastal and river flood risk analyses for guiding economically optimal flood adaptation policies: A country-scale study for mexico. *Philos Trans A Math Phys Eng Sci* 376, no 2121.

- Hall, T.M. and A.H. Sobel. 2013. On the impact angle of hurricane sandy's new jersey landfall. *Geophysical Research Letters* 40, no 10: 2312-15.
- Hartnett, M. and S. Nash. 2017. High-resolution flood modeling of urban areas using msn_flood. *Water Science and Engineering* 10, no 3: 175-83.
- Horritt, M.S. and P.D. Bates. 2001a. Effects of spatial resolution on a raster based model of flood flow. *Journal of Hydrology* 253, no 1: 239-49.
- Horritt, M.S. and P.D. Bates. 2001b. Predicting floodplain inundation: Raster-based modelling versus the finite-element approach. *Hydrological Processes* 15, no 5: 825-42.
- Horritt, M.S. and P.D. Bates. 2002. Evaluation of 1d and 2d numerical models for predicting river flood inundation. *Journal of Hydrology* 268, no 1: 87-99.
- Jevrejeva, S., L.P. Jackson, R.E. Riva, A. Grinsted and J.C. Moore. 2016. Coastal sea level rise with warming above 2 degrees c. *Proc Natl Acad Sci U S A* 113, no 47: 13342-47.
- Kantha, L.H. and C.A. Clayson. 2000. *Numerical models of oceans and oceanic processes*: Elsevier Science. https://books.google.co.uk/books?id=w-Muo8D_EAMC
- Kumbier, K., R.C. Carvalho, A.T. Vafeidis and C.D. Woodroffe. 2018. Investigating compound flooding in an estuary using hydrodynamic modelling: A case study from the shoalhaven river, australia. *Natural Hazards and Earth System Sciences* 18, no 2: 463-77.
- Leon, J.X., G.B.M. Heuvelink and S.R. Phinn. 2014. Incorporating dem uncertainty in coastal inundation mapping. *PLOS ONE* 9, no 9: e108727.
- Lewis, M., P. Bates, K. Horsburgh, J. Neal and G. Schumann. 2013. A storm surge inundation model of the northern bay of bengal using publicly available data. *Quarterly Journal of the Royal Meteorological Society* 139, no 671: 358-69.
- Li, J. and D.W.S. Wong. 2010. Effects of dem sources on hydrologic applications. *Computers, Environment and Urban Systems* 34, no 3: 251-61.
- Lin, N. and K. Emanuel. 2015. Grey swan tropical cyclones. *Nature Climate Change* 6, no 1: 106-11.
- Mattocks, C. and C. Forbes. 2008. A real-time, event-triggered storm surge forecasting system for the state of north carolina. *Ocean Modelling* 25, no 3-4: 95-119.
- Mcclatchey, J., R. Devoy, D. Woolf, B. Bremner and N. James. 2014. Climate change and adaptation in the coastal areas of europe's northern periphery region. *Ocean & Coastal Management* 94: 9-21.

- Mcgranahan, G., D. Balk and B. Anderson. 2007. The rising tide: Assessing the risks of climate change and human settlements in low elevation coastal zones. *Environment and Urbanization* 19, no 1: 17-37.
- Mennel, E. Have we been overestimating flood risk on the outer banks? <http://wunc.org/post/have-we-been-overestimating-flood-risk-outer-banks#stream/0>.
- N.C.E.I. Ncei hurricane sandy digital elevation models. https://www.ngdc.noaa.gov/mgg/inundation/sandy/sandy_geoc.html.
- N.O.A.A. Atlantic city, nj - station id: 8534720. <https://tidesandcurrents.noaa.gov/stationhome.html?id=8534720>.
- Neal, J., G. Schumann, T. Fewtrell, M. Budimir, P. Bates and D. Mason. 2011. Evaluating a new lisflood-fp formulation with data from the summer 2007 floods in tewkesbury, uk. *Journal of Flood Risk Management* 4, no 2: 88-95.
- Nicholls, R.J. and A. Cazenave. 2010. Sea-level rise and its impact on coastal zones. *Science* 328, no 5985: 1517-20.
- Nikolakopoulos, K.G., E.K. Kamaratakis and N. Chrysoulakis. 2006. Srtm vs aster elevation products. Comparison for two regions in crete, greece. *International Journal of Remote Sensing* 27, no 21: 4819-38.
- Planet, T. Planet application program interface: In space for life on earth. <https://api.planet.com/>.
- Quinn, N., M. Lewis, M.P. Wadey and I.D. Haigh. 2014. Assessing the temporal variability in extreme storm-tide time series for coastal flood risk assessment. *Journal of Geophysical Research: Oceans* 119, no 8: 4983-98.
- Rosner, A., R.M. Vogel and P.H. Kirshen. 2014. A risk-based approach to flood management decisions in a nonstationary world. *Water Resources Research* 50, no 3: 1928-42.
- Saghafian, B., S. Golian and A. Ghasemi. 2013. Flood frequency analysis based on simulated peak discharges. *Natural Hazards* 71, no 1: 403-17.
- Savage, J.T.S., P. Bates, J. Freer, J. Neal and G. Aronica. 2016. When does spatial resolution become spurious in probabilistic flood inundation predictions? *Hydrological Processes* 30, no 13: 2014-32.
- Seenath, A. 2015. Modelling coastal flood vulnerability: Does spatially-distributed friction improve the prediction of flood extent? *Applied Geography* 64: 97-107.

- Seenath, A., M. Wilson and K. Miller. 2016. Hydrodynamic versus gis modelling for coastal flood vulnerability assessment: Which is better for guiding coastal management? *Ocean & Coastal Management* 120: 99-109.
- Siegrist, M. and H. Gutscher. 2006. Flooding risks: A comparison of lay people's perceptions and expert's assessments in switzerland. *Risk Anal* 26, no 4: 971-9.
- Spasojevic, M. and M.H. Forrest. 2008. Two- and three-dimensional numerical solution of mobile-bed hydrodynamics and sedimentation. . In *Sedimentation engineering: Processes, measurements, modeling, and practice.* , ed. Garcia, MH, 683-762. Virginia: American Society of Civil Engineers.
- Vaze, J., J. Teng and G. Spencer. 2010. Impact of dem accuracy and resolution on topographic indices. *Environmental Modelling & Software* 25, no 10: 1086-98.
- Verwaest, T., K.V.D. Biest, P. Vanpoucke, J. Reyns, P. Vanderkimpen, L.D. Vos, J.D. Rouck and T. Mertens. 2012. Coastal flooding risk calculations for the belgian coast. In *Coastal engineering 2008*, 4193-201: World Scientific Publishing Company.
- Viglione, A., G. Di Baldassarre, L. Brandimarte, L. Kuil, G. Carr, J.L. Salinas, A. Scolobig and G. Blöschl. 2014. Insights from socio-hydrology modelling on dealing with flood risk – roles of collective memory, risk-taking attitude and trust. *Journal of Hydrology* 518: 71-82.
- Vousdoukas, M.I., E. Voukouvalas, L. Mentaschi, F. Dottori, A. Giardino, D. Bouziotas, A. Bianchi, P. Salamon and L. Feyen. 2016. Developments in large-scale coastal flood hazard mapping. *Natural Hazards and Earth System Sciences* 16, no 8: 1841-53.
- Wadey, M.P., R.J. Nicholls and I. Haigh. 2013. Understanding a coastal flood event: The 10th march 2008 storm surge event in the solent, uk. *Natural Hazards* 67, no 2: 829-54.
- Waters, C.N., J. Zalasiewicz, C. Summerhayes, A.D. Barnosky, C. Poirier, A. Galuszka, A. Cearreta, M. Edgeworth, E.C. Ellis, M. Ellis, C. Jeandel, R. Leinfelder, J.R. McNeill, D. Richter, W. Steffen, J. Syvitski, D. Vidas, M. Waprich, M. Williams, A. Zhisheng, J. Grinevald, E. Odada, N. Oreskes and A.P. Wolfe. 2016. The anthropocene is functionally and stratigraphically distinct from the holocene. *Science* 351, no 6269: aad2622.
- Zhang, J., P. Atkinson and M.F. Goodchild. 2014. *Scale in spatial information and analysis*: Taylor & Francis. <https://books.google.co.uk/books?id=mOgxAwAAQBAJ>
- Zhang, Y.J. and A.M. Baptista. 2008. An efficient and robust tsunami model on unstructured grids. Part i: Inundation benchmarks. *Pure and Applied Geophysics* 165, no 11-12: 2229-48.

Tables

Table 1. Statistical descriptors of each re-gridded DEM.

DEM		Elevation characteristics (m)				Error (m)		
Resolution	Minimum	Maximum	Mean	Standard Deviation	ME*	SE**	RMSE***	
10	-12.95	8.01	-3.58	4.31	-	-	-	
15	-12.89	7.46	-3.55	4.30	0.019	0.007	0.113	
20	-12.73	7.08	-3.54	4.30	-0.001	0.010	0.148	
30	-12.29	6.50	-3.54	4.30	-0.061	0.037	0.594	
40	-12.77	6.64	-3.55	4.30	-0.021	0.040	0.633	
50	-11.97	6.36	-3.54	4.30	0.0170	0.022	0.350	
100	-12.49	4.62	-3.56	4.30	-0.061	0.061	0.966	

*Mean error (ME) relative to the 10 m DEM.
**Standard error (SE) relative to the 10 m DEM.
***Root mean squared error (RMSE) relative to the 10 m DEM.

Table 2. Percentage change in area inundated relative to DEM resolution

DEM Resolution (m)	Inundated area (%)		Percentage change*	
	Tidal cycle	Storm surge	Tidal cycle	Storm surge
10	65.55	66.40	-	-
15	65.64	66.49	0.13	0.13
20	65.91	66.76	0.55	0.54
30	65.34	66.21	-0.32	-0.29
40	65.24	66.07	-0.47	-0.49
50	65.56	66.38	0.01	-0.03
100	65.80	66.64	0.38	0.36

* Percentage change calculated using area inundated from the 10 m DEM as the baseline for comparison.

Table 3. Statistical comparison of the differences between the observed and predicted flood extents relative to DEM resolution.

Statistic*	DEM resolution (m)						
	10	15	20	30	40	50	100
Standard error (m)	0.38	0.46	0.53	0.71	0.93	1.01	2.13
RMSE (m)	29.08	29.26	29.99	35.57	41.20	39.30	90.28
Mean absolute error (m)	23.68	24.04	25.03	28.62	35.79	34.17	85.54

*Error statistics were based on the estimated distance between the predicted and observed flood extent indicators.

Figure Caption List

Figure 1. Overview of the application site location. (Sources: National Geographic, Esri, DeLorme, HERE, UNEP-WCMC, USGS, NASA, ESA, METI, NRCAN, GEBCO, NOAA, increment P Corp.)

Figure 2. Source coastal elevation model used in the re-gridding process to produce DEMs at coarser resolution. (Sources: National Geographic, Esri, DeLorme, HERE, UNEP-WCMC, USGS, NASA, ESA, METI, NRCAN, GEBCO, NOAA, increment P Corp.)

Figure 3. Time series plot of the observed 24-hour tidal cycle and storm surge scenario created. The storm surge scenario was generated by superimposing a 1.5 m storm surge onto the 24-hour tidal cycle, which was obtained from NOAA's Atlantic City tide gauge station. Highest water elevation generated in this process was 1.92 m above NAVD88.

Figure 4. Cross-sections of all re-gridded DEMs showing profiles from the ocean through beach to higher ground characteristic of the application site. From these, it is clear that there are prominent slope characteristics, which may be the key control on flood flow at the study site.

Figure 5. Comparison of inundation extent from the (a) 24-hour tidal cycle and (b) storm surge scenario relative to DEM resolution. (Sources: National Geographic, Esri, DeLorme, HERE, UNEP-WCMC, USGS, NASA, ESA, METI, NRCAN, GEBCO, NOAA, increment P Corp.)

Figure 6. Schematic diagram illustrating how the distance between the predicted flood extent points and the observed flood extent line was estimated in ArcMap 10.3.1.

Figure 7. Elevation characteristics of each re-gridded DEM. From the box plot, it is clear that the re-gridding procedure had little impact on the overall quality and topographic complexity of the re-sampled DEMs. This can be related to the terrain slope characteristics of the area.

Figure 8. A comparison of the elevation differences between the coarser DEMs and the 10 m DEM (i.e. the finest resolution used in the model). Again, it is shown that the nearest neighbour re-gridding procedure applied had minimal impact on the final quality and topographic complexity of the re-gridded DEMs.

Figure 9. Elevation characteristics of (a) the 30 m and (b) 50 m DEMs created using the nearest neighbour, bilinear, and cubic convolution interpolation methods. Here, it is shown that there were no differences in the DEMs generated from all three interpolation methods. Therefore, the flood model outputs derived from the nearest neighbour re-gridded DEMs are not likely to differ from those that would have been generated using a bilinear or cubic convolution smoothing algorithm.

Figure 10. RMSE in coastal flood extent predictions obtained from (a) each re-gridded DEM and (b) projecting water levels predicted from the coarser DEMs ($\geq 15\text{m}$) onto the 10 m DEM. The spike seen in the graph at 40 m is related to the quality of the 40 m DEM. From Figure 8, it is noted that the 50 m DEM had a slightly better fit with the 10 m DEM. Therefore, the RMSE of the flood-extent predictions generated from the 40 m DEM was slightly higher than the RMSE of the flood-extent predictions obtained from the 50 m DEM.

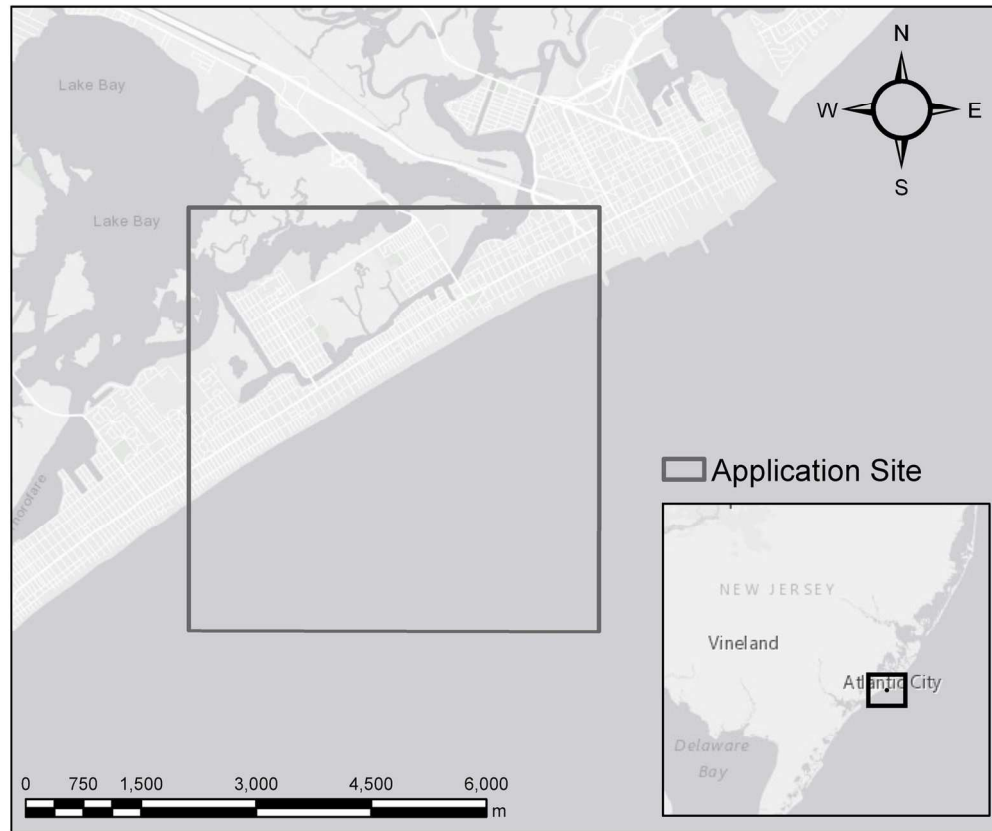


Figure 1. Overview of the application site location. (Sources: National Geographic, Esri, DeLorme, HERE, UNEP-WCMC, USGS, NASA, ESA, METI, NRCAN, GEBCO, NOAA, increment P Corp.)

146x122mm (300 x 300 DPI)

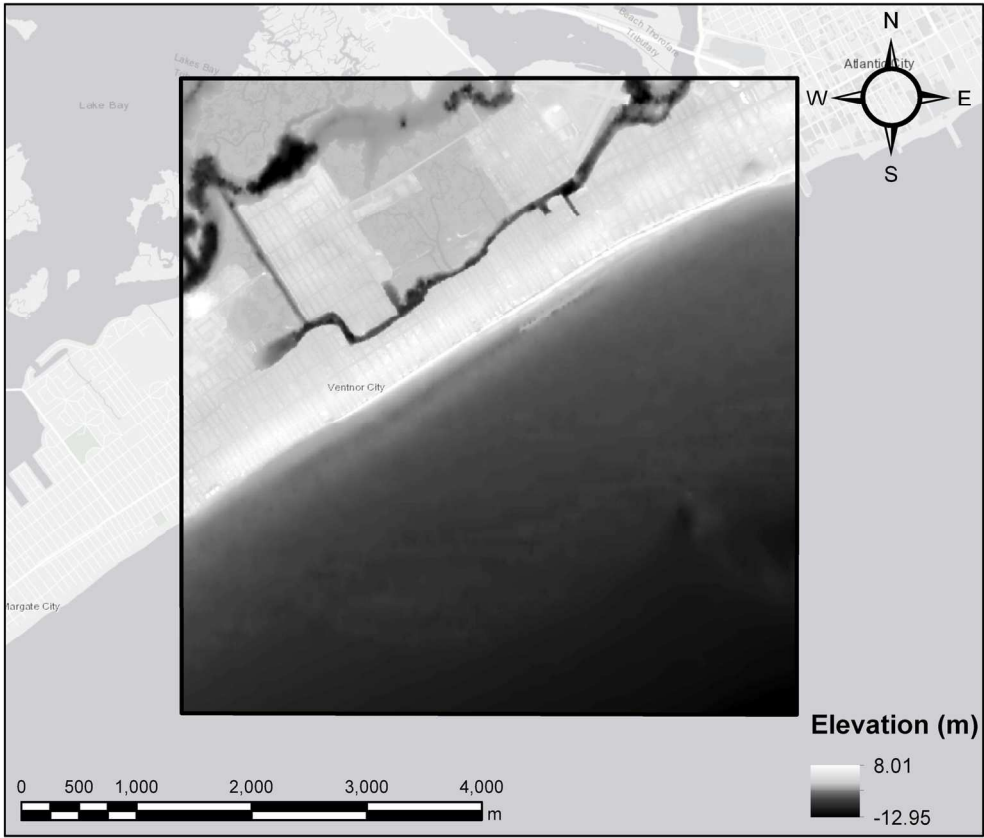


Figure 2. Source coastal elevation model used in the re-gridding process to produce DEMs at coarser resolution. (Sources: National Geographic, Esri, DeLorme, HERE, UNEP-WCMC, USGS, NASA, ESA, METI, NRCAN, GEBCO, NOAA, increment P Corp.)

147x125mm (300 x 300 DPI)

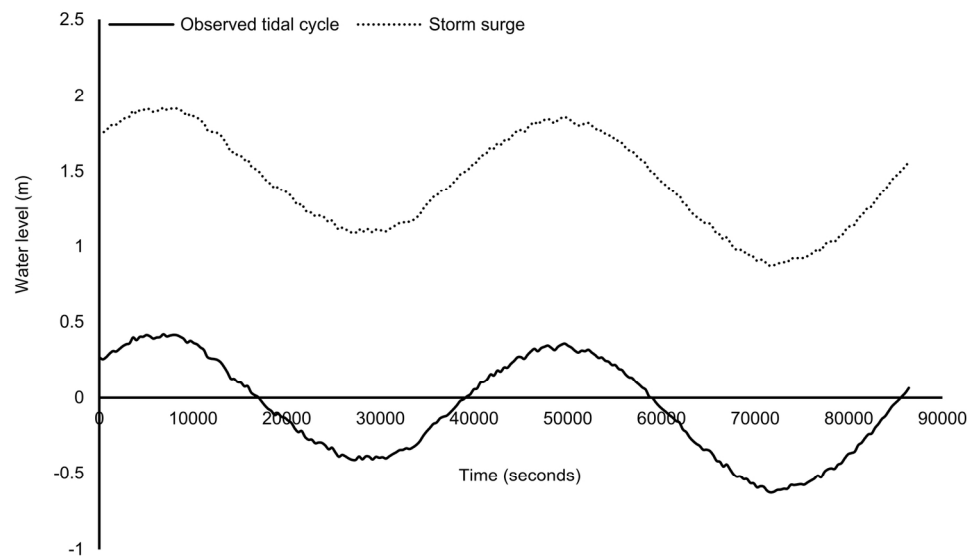


Figure 3. Time series plot of the observed 24-hour tidal cycle and storm surge scenario created. The storm surge scenario was generated by superimposing a 1.5 m storm surge onto the 24-hour tidal cycle, which was obtained from NOAA's Atlantic City tide gauge station. Highest water elevation generated in this process was 1.92 m above NAVD88.

79x45mm (600 x 600 DPI)

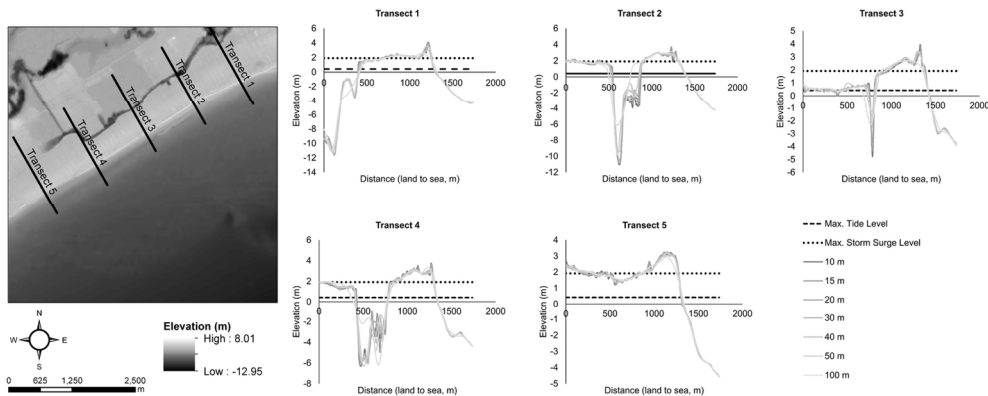


Figure 4. Cross-sections of all re-gridded DEMs showing profiles from the ocean through beach to higher ground characteristic of the application site. From these, it is clear that there are prominent slope characteristics, which may be the key control on flood flow at the study site.

136x56mm (300 x 300 DPI)

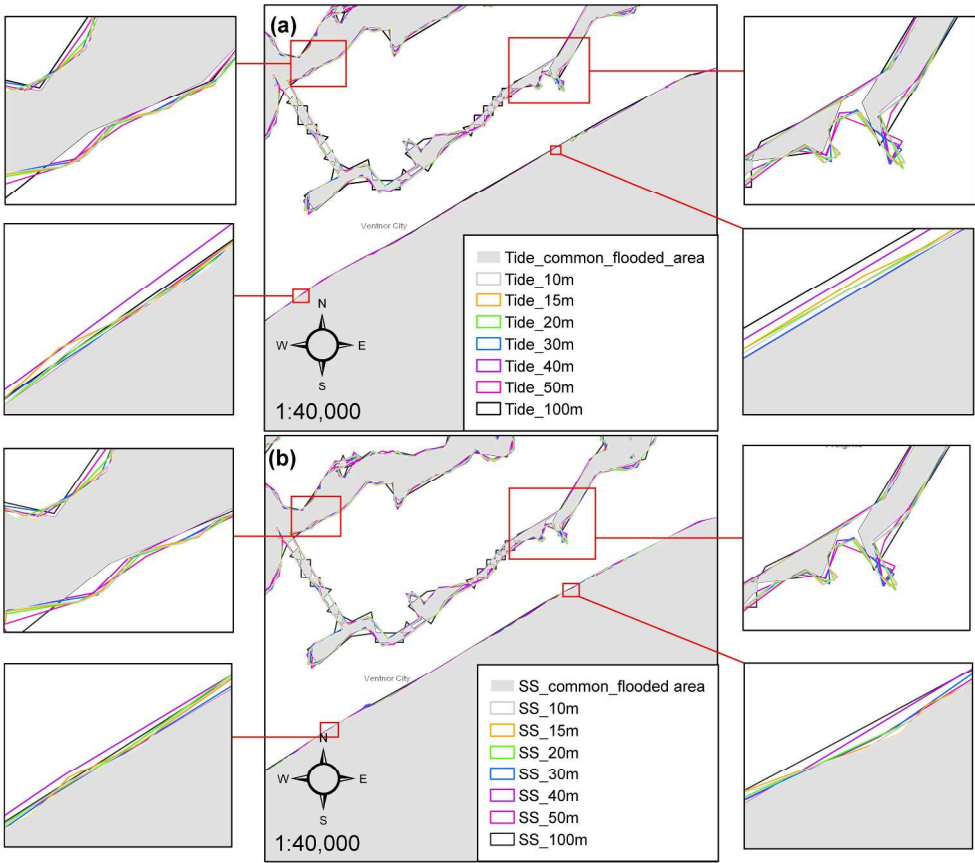


Figure 5. Comparison of inundation extent from the (a) 24-hour tidal cycle and (b) storm surge scenario relative to DEM resolution. (Sources: National Geographic, Esri, DeLorme, HERE, UNEP-WCMC, USGS, NASA, ESA, METI, NRCAN, GEBCO, NOAA, increment P Corp.)

234x202mm (300 x 300 DPI)

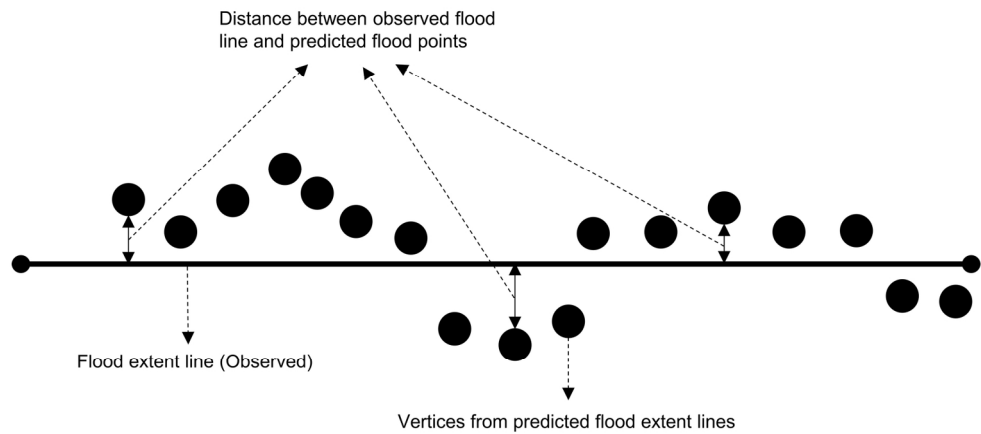


Figure 6. Schematic diagram illustrating how the distance between the predicted flood extent points and the observed flood extent line was estimated in ArcMap 10.3.1.

79x37mm (600 x 600 DPI)

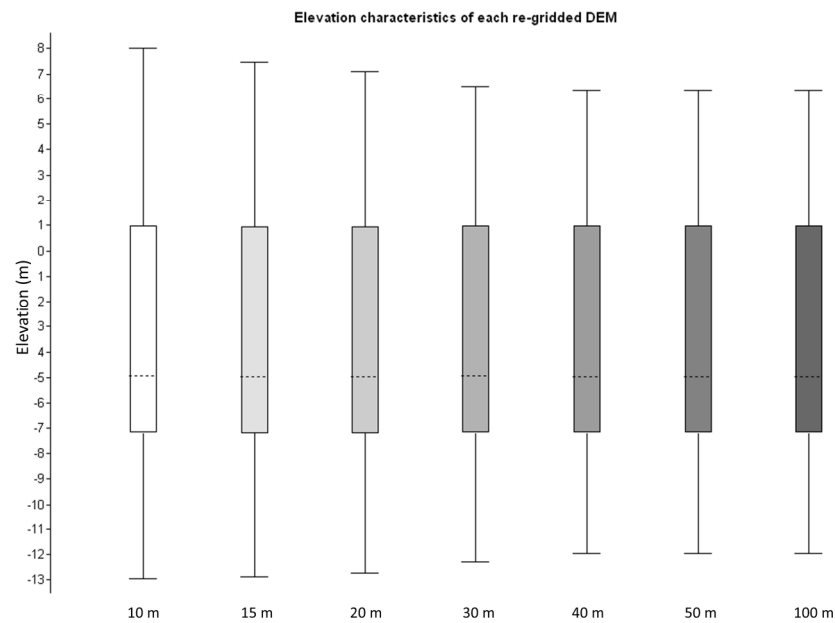


Figure 7. Elevation characteristics of each re-gridded DEM. From the box plot, it is clear that the re-gridding procedure had little impact on the overall quality and topographic complexity of the re-sampled DEMs. This can be related to the terrain slope characteristics of the area.

190x120mm (300 x 300 DPI)

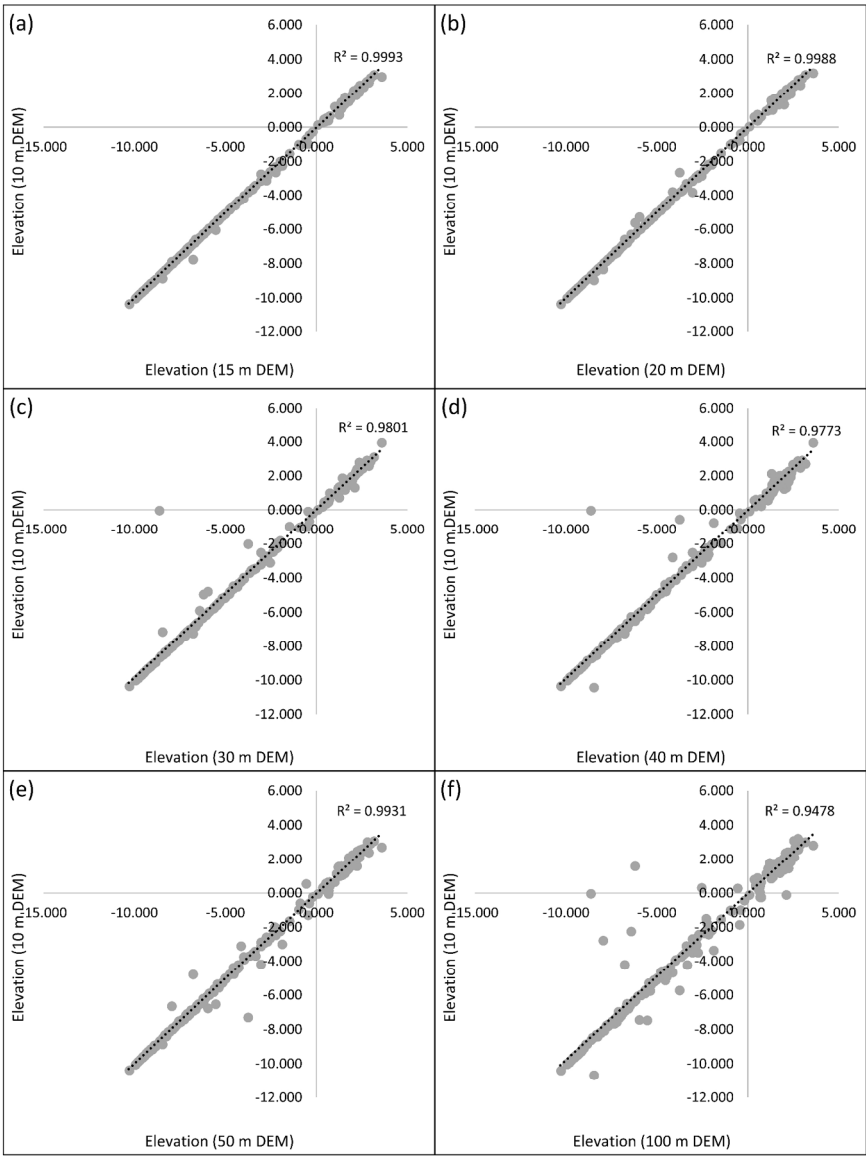


Figure 8. A comparison of the elevation differences between the coarser DEMs and the 10 m DEM (i.e. the finest resolution used in the model). Again, it is shown that the nearest neighbour re-gridding procedure applied had minimal impact on the final quality and topographic complexity of the re-gridded DEMs.

249x328mm (300 x 300 DPI)

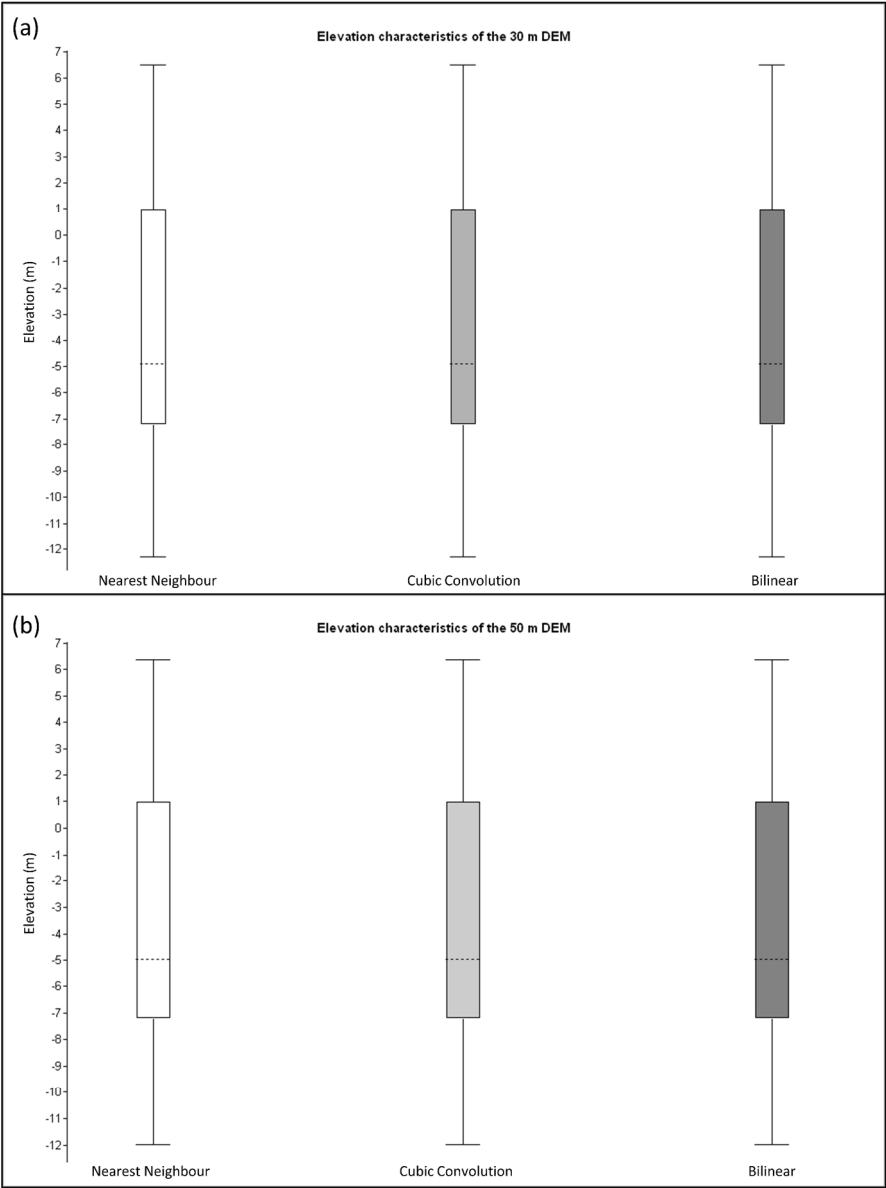


Figure 9. Elevation characteristics of (a) the 30 m and (b) 50 m DEMs created using the nearest neighbour, bilinear, and cubic convolution interpolation methods. Here, it is shown that there were no differences in the DEMs generated from all three interpolation methods. Therefore, the flood model outputs derived from the nearest neighbour re-gridded DEMs are not likely to differ from those that would have been generated using a bilinear or cubic convolution smoothing algorithm.

279x372mm (300 x 300 DPI)

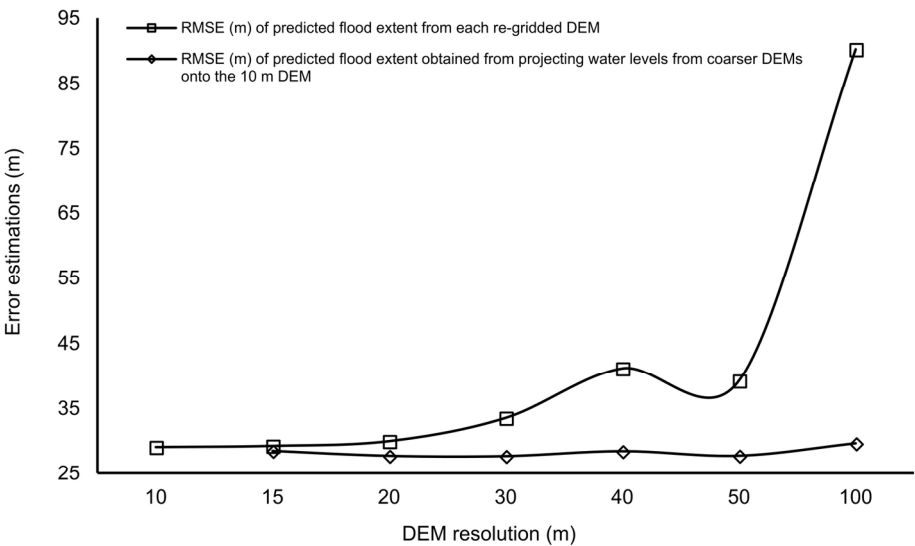


Figure 10. RMSE in coastal flood extent predictions obtained from (a) each re-gridded DEM and (b) projecting water levels predicted from the coarser DEMs ($\geq 15\text{m}$) onto the 10 m DEM. The spike seen in the graph at 40 m is related to the quality of the 40 m DEM. From Figure 8, it is noted that the 50 m DEM had a slightly better fit with the 10 m DEM. Therefore, the RMSE of the flood-extent predictions generated from the 40 m DEM was slightly higher than the RMSE of the flood-extent predictions obtained from the 50 m DEM.

79x45mm (600 x 600 DPI)